Dynamic Analysis of three Voltage Source Power Converters supplying Squirrel Cage Induction Machines

F.D. Kanellos, N.D. Hatziargyriou

Dept. of Electrical and Computer Engineering, National Technical University of Athens,
Zografou, 15773, Greece (e-mail: kanellos@power.ece.ntua.gr, nh@power.ece.ntua.gr)

Abstract – In this paper, the dynamic analysis of three of the most promising types of voltage source converters, is studied. The converters supply squirrel cage induction machines and they employ hysteresis current control, voltage space vector modulation and sinusoidal pulse width modulation (SPWM), respectively. Detailed models for the electrical drives are used, allowing the study of their behavior in a broad bandwidth. The presented models are developed using Matlab code and Simulink. Indirect field-oriented control is used for the regulation of the rotating speed and the stator flux. The hysteresis current controller is composed of three independent per phase current controllers. DC side is considered ideal as it is assumed that the control system maintains the dc voltage at its reference value. The operational characteristics of the examined variable speed schemes are studied using their response to step changes of the load torque and the reference speed.

Keywords – Control, PWM, vector control, induction machines, space vectors, hysteresis current control, harmonics, switching frequencies.

I. INTRODUCTION

The recent evolution in power electronics [1],[2], the associated new modulation techniques and the microprocessors [3],[4], facilitated the application of sophisticated control techniques ensuring better operational characteristics of the variable frequency drives. AC induction machine drives now compare favorably to DC motor drives, on considerations such as power to weight ratio, acceleration performance, maintenance, operating environment and higher operating speed without mechanical commutator. Cost and robustness of the machine and control flexibility are often reasons for choosing induction machine drives in small to medium power range applications. Field-oriented and torque control [3]-[5],[7] techniques render the induction machines possibly the main choice for variable speed drives in the future.

In a typical induction motor drive, the power converter serves to convert the supplied energy into a form suited for the operation of the motor. The power converter conditions the power delivered to the motor in some desired manner directed by the controller. The primary function of the controller is to translate the command value and feedback signals to control signals for operating the converter. Inverter types can be divided into two broad categories by the source characteristic of their dc links: voltage or current source inverters. Most of today's small induction motor drives use voltage source pulse-width-modulation (PWM) [5],[6],[8] inverter that allows for both magnitude and frequency of its output voltages to be changed electronically.

The function of the pulse-width modulator is to translate the modulation waveforms into a train of switching pulses for the inverter.

In the following, the dynamic analysis of three of the most promising types of voltage source converters, is studied. The converters supply squirrel cage induction machines and they employ hysteresis current control [6],[9], voltage space vector modulation, sinusoidal pulse width modulation (SPWM), respectively. The hysteresis current controller is composed of three independent per phase current controllers. Indirect field-oriented control [3],[6],[9]-[11] is used for the regulation of the rotating speed and the stator flux. Two PI controllers are used for the tracking of the optimal *dq*-axis current. In case of stationary frame PI regulator a cross-coupling term is very useful. In the present study a synchronous frame PI regulator is used. In case of the converter employing hysteresis technique the tracking of the current reference does not require the use of PI controllers. The main advantage of this method is the accurate tracking of the current reference and consequently its high dynamic performance.

Most of the published models of electrical drives consider only the fundamental voltage component for the study of fast transients. In this paper detailed and fully parametric models for the power electronics and the induction machine are used, allowing the study of their behavior in a broad area of switching frequencies. The presented models are developed using Matlab code and Simulink that further facilitates the accurate design and evaluation of the examined schemes.

The response of the examined variable speed schemes in the extreme case of simultaneous step changes of the load and the reference speed, is studied. Using the results obtained the operational characteristics of the proposed variable speed schemes are evaluated. Results relative with the spectral density of the electromagnetic torque are obtained. These results can be used in order to detect possible mechanical resonances. The propagated harmonics to the stator currents that represent machine ohmic losses are also calculated.

II. MODEL OF THE IM DRIVE

In this section the detailed models of the IM, the control system and the modulation techniques are briefly reviewed.
  The connection of the induction machine to the grid is achieved via a voltage source converter cascade, as shown in Fig. 1, in order to control the reactive power exchanged

between the network and the electrical machine and also to provide variable speed mode of operation.
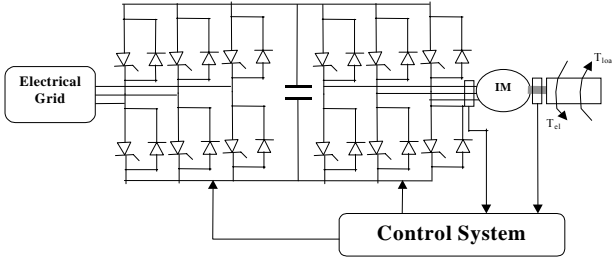

Fig.1 DVS converter cascade

A. Induction Machine Model

Induction machines are represented by the fourth order model expressed in the arbitrary reference frame [10],[12]. Using generator convention for the stator currents the *dq*-stator and rotor voltages are given by

$$u_{sd} = -r_s \cdot i_{sd} - \omega \cdot \Psi_{sq} + p\Psi_{sd}$$

$$u_{sq} = -r_s \cdot i_{sq} + \omega \cdot \Psi_{sd} + p\Psi_{sq} \qquad (1)$$

$$u_{rd} = 0 = r_r \cdot i_{rd} - (\omega - \omega_r) \cdot \Psi_{rq} + p\Psi_{rd}$$

$$u_{rq} = 0 = r_r \cdot i_{rq} + (\omega - \omega_r) \cdot \Psi_{rd} + p\Psi_{rq}$$

Where $p = \dfrac{1}{\omega_o}\dfrac{d}{dt}$, ω_o is the base cyclic frequency, ω is the rotating speed of the arbitrary reference frame and subscripts {d}, {q}, {s}, {r} denote d,q-axis, stator, rotor, respectively.

The fluxes are related to the winding currents by the following equations,

$$\Psi_{sd} = -X_s \cdot i_{sd} + X_m \cdot i_{rd}$$

$$\Psi_{sq} = -X_s \cdot i_{sq} + X_m \cdot i_{rd}$$

$$\Psi_{rd} = -X_m \cdot i_{sd} + X_r \cdot i_{rd} \qquad (2)$$

$$\Psi_{rq} = -X_m \cdot i_{sq} + X_r \cdot i_{rq}$$

The equivalent of the n elastically connected masses [10] can be optionally used for simulating the mechanical system of the electrical drive.

In the reported simulations the following simple equation of the mechanical system is adopted.

$$J \frac{d\omega_r}{dt} = T_{el} - T_l - k \cdot \omega_r \qquad (3)$$

Where ω_r is the angular rotating speed, J is the inertia and k is the damping factor. Subscripts {r}, {el}, {l} denote rotor, electromagnetic and mechanical load, respectively.

B. IM Control

The generator control system consists of two major loops, one for the rotor rotating speed and the other for the rotor flux linkage. In Fig.2 the production of the speed and flux references from load torque and measured rotating speed is shown. The field weakening and load –speed characteristics together with a low pass filter (T=0.01 sec) are used. The measured load signal is led to the load–optimal rotating speed characteristic, which produces the input signal to a low-pass filter of a 0.01sec time-constant. The output of the low-pass filter is fed next as input to the rotating speed controller. So optimal performance is achieved by tracking the optimal rotating speed. At high loads the control scheme imposes a constant rotating speed. As mentioned before, the desired electromagnetic torque is achieved by the application of a field-orientation control scheme.
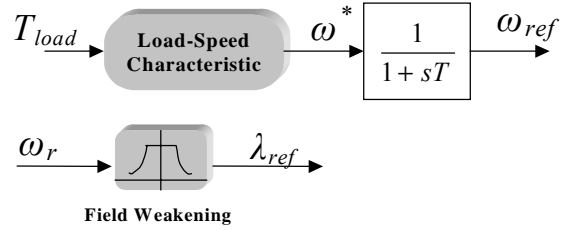

Fig.2 Production of the speed and flux references

Knowing the value of the desired electromagnetic torque T_{em}^{*}, the *q*-axis current component in the field-oriented frame is given by the equation [3],[10],

$$I_{qs}^{e*} = \frac{4 L_r' T_{em}^{*}}{3 PL_m \lambda_{dr}^{'e*}} \qquad (4)$$

Superscripts {*}, {e} denote the reference value and the field oriented frame, respectively.

It is also known that, when properly oriented, the slip speed and the dq-axis current components in the field oriented frame are related as [3],[10],

$$\omega^{*} = \omega_e - \omega_r = \frac{r_r}{L_r} \frac{I_{qs}^{e*}}{I_{ds}^{e*}} \qquad (5)$$

Rotor flux can be controlled by regulating I_{ds}^{e}. Given some desired level of the rotor flux, the desired value of the d-axis current component can be obtained from [3],[11]:

$$I_{ds}^{e*} = \frac{r_r + L_r p}{r_r L_m} \lambda_{dr}^{e} \qquad (6)$$

C. Indirect Field-Oriented Voltage Control

The desired *dq*-axis voltages in the field-oriented frame are traditionally obtained from the fourth order model of the induction machine. The only drawback of this control scheme is that it requires accurate knowledge of the machine parameters. It is commonly used with on-line parameter adaptive techniques for tuning the value of the parameters used in the indirect field controller, ensuring in this way successful operation. A modification of the method leads to the use of two PI controllers for the tracking of the optimal *dq*-axis current [3],[6],[13]-[15]and it is

depicted in Fig. 3. In case of stationary frame PI regulator a cross-coupling term is very useful. In the present study a synchronous frame PI regulator is used, as shown in Fig. 3.

D. Indirect Field-Oriented Current Control using Hysteresis Technique

In case Indirect Field-Oriented Current Controlled IM using hysteresis current control the PI current Controllers do not apply. The exact tracking of the reference value of the stator currents is achieved by the application of a hysteresis current controller, which is described in more detail in subsection G. This method ensures high dynamic performance but gives rise to the problem of the higher switching frequencies and the generation of subharmonic components. It does not also adequately ensure the maintenance of the current inside the hysteresis band as a maximum error of twice the hysteresis band occurs on a random basis.
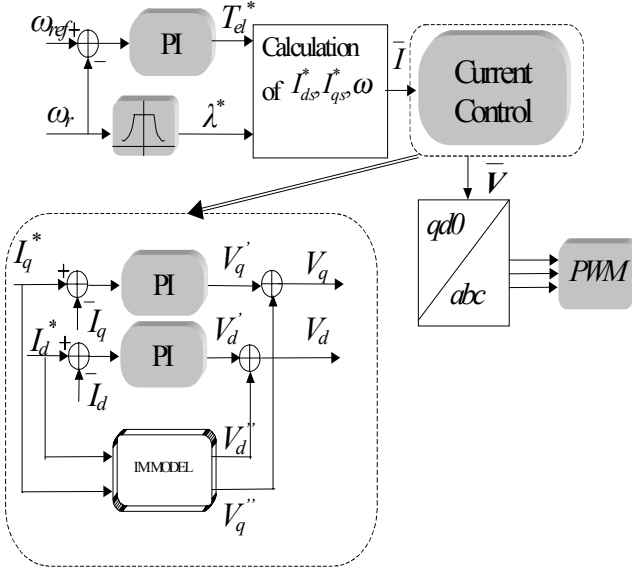

Fig. 3 Indirect field-oriented voltage controller

E. Sinusoidal Pulse Width Modulation

This method employs individual carrier modulators in each of the three phases [5],[6],[8],[10]. The reference signals U_a^*, U_b^*, U_c^* of the phase voltages are sinusoidal in the steady state, forming a symmetrical three-phase system. They are obtained from the reference vector U^*, which is split into its three phase components U_a^*, U_b^*, U_c^*. Three comparators and a triangular carrier signal U_{cr}, which is common to all three-phase signals, generate the logic signals U_a', U_b', and U_c' that control the half-bridges of the power converter.

This method does not fully utilize the available *DC* voltage. The maximum value of the modulation index, *0.785*, is reached at a point where the amplitudes of the reference signal and the carrier become equal. The maximum line-to-line voltage amplitude in this operating point is

$$U_a^*(t_1) - U_b^*(t_1) = \sqrt{3}U_d / 2 \qquad (7)$$

This is less than what is obviously possible when e.g. the phases *a* and *b* are switched to $U_a = U_d/2$ and $U_b = -U_d/2$, respectively. In this case, the maximum line-to-line voltage would equal U_d.

The aforementioned method operates at constant carrier frequency, while the fundamental frequency is permitted to vary. The switching frequency is then nonperiodic in principle and the corresponding Fourier spectra are continuous containing frequencies lower than the lowest carrier sideboard. These harmonics are undesired and produce low-frequency torque harmonics [16]-[18] that may stimulate resonances in the mechanical transmission train of the drive system. A synchronization between the carrier frequency and the controlling fundamental avoids these drawbacks. A reduction of the harmonic distortion can be achieved by adding zero-sequence waveforms to the sinusoidal reference signal.

F. Space Vector Modulation

The space vector modulation technique [6],[8],[19] differs from the aforementioned method in that there are not separate modulators used for each the three phases. Instead. the complex reference voltage vector is processed as a whole. The switching vectors and the voltage reference are shown in Fig.4 [6],[8]. Also the boundaries between the controllable range, the six-step operation and overmodulation are shown in the same figure.
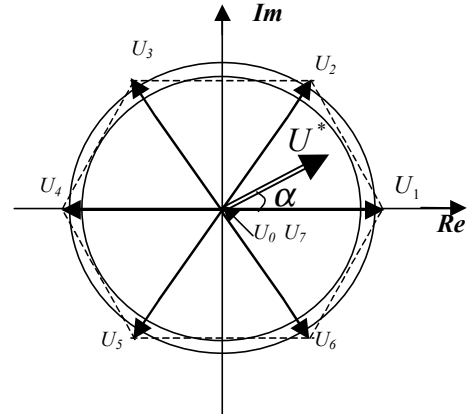

Fig. 4 Voltage reference and switching-state vectors

The reference vector U^* is sampled at a fixed frequency $2f_s$. The sampled value $U^*(t_s)$ is then used to solve the equations:

$$2f_s \cdot (t_a U_a + t_b U_b) = U^*(t_s)$$
$$t_0 = \frac{1}{2f_s} - t_a - t_b \qquad (8)$$

Where U_a and U_b are the two switching-state vectors

adjacent in space to the reference vector U^*. The solutions of equation (8) are the respective on-durations t_a, t_b, and t_o of the switching-state vectors U_a, U_b, U_o:

$$t_a = \frac{3}{2\pi f_s} U^*(t_s)(\cos \alpha - \frac{1}{\sqrt{3}} \sin \alpha)$$

$$t_b = \frac{2\sqrt{3}}{2\pi f_s} U^*(t_s) \sin \alpha \qquad (9)$$

$$t_0 = \frac{1}{2 f_s} - t_a - t_b$$

The angle α in these equations is the phase angle between the reference vector and U_a.

This technique in effect averages the three switching-state vectors over a sub-cycle interval $t_o = 1/2f_s$ to equal the reference vector $U^*(t_s)$ as sampled at the beginning of the sub-cycle. It is assumed in Fig. 4 that the reference vector is located in the first 60° sector of the complex plane. The switching-state vectors adjacent to the reference vector are then U_1 and U_2. As the reference vector enters the next sector, U_2 and U_3, compose the reference voltage vector.

Having computed the on-durations of the three switching-state vectors that form one subcycle, an adequate sequence in time of these vectors must be determined next. The zero vector is redundant. It can be either formed as $U_o(---)$ or $U_7(+++)$. U_o is preferred when the previous switching-state vector is U_1, U_3 or U_5 while U_7 will be chosen following U_2, U_4, U_6. This ensures that only one half-bridge needs to commutate at a transition between an active switching-state vector and the zero vector. Hence, the minimum number of commutations is obtained.

G. Hysteresis Current Control

The behavior of this kind of controller can be explained in terms of complex plane switching diagram shown in Fig. 5 [6]-[8]. The switching lines are located at a distance h, equal to the hysteresis band, from the tip of the current reference vector. The entire diagram moves with the current reference vector with its center remaining fixed at the tip of the vector.
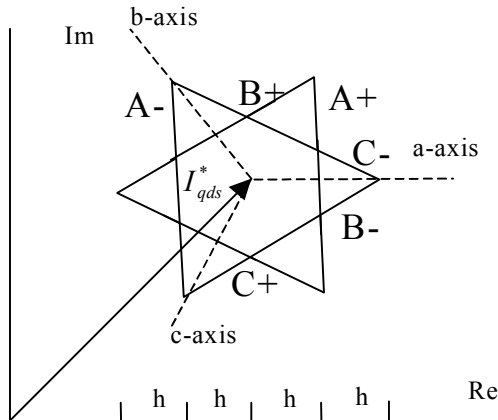

Fig. 5 Switching diagram

The typical or expected behavior of the controller is to confine operation to the interior, hexagonal region of the switching diagram. Thus, whenever the current error touches one of the switching lines, that inverter leg is switched driving the current error in that leg in the opposite direction. Note, however, that the current error can be carried to one of the switching lines by motion of the current vector I_{qds}^s or by motion of the current reference vector I_{qds}^{s*} and the attached switching diagram. Thus, the situation occurs, where, for example, the (A-) switching line is encountered with the inverter in the state (a+,b-,c-). The system is then effectively short-circuited and can "coast" out to the tip of the switching diagram before a new switching of the inverter occurs. During this period the motor is effectively "out of control" since the exact trajectory is determined only by the motor parameters and the internal E.M.F. at this condition and not by the applied voltages. Hence, an error of $2\Delta I_s$, twice the expected value equal to the hysteresis band, can occur on an almost random basis. This problem can be overcome by incorporating a second threshold that senses when the boundary is being reached with the inverter in a state that would produce a short-circuited condition and avoiding this mode.

One of the main drawbacks of this method is that there is a tendency to lock into limit cycles of high frequency switching which comprise only nonzero voltage vectors. Clocking and controlling the switching frequency can remedy this. Also the modulation process generates subharmonics increasing the mechanical stresses and the possibility of undesirable mechanical resonances. The current error is not strictly limited while the maximum overshoot is twice the width of the hysteresis band.

III. RESULTS

In this section the results obtained by the simulation of the aforementioned models are given. The induction machine is assumed to operate with a constant load of 0.5 p.u. At $t=0.5sec$ a step change of the load from 0.5 p.u. to 0.7 p.u. occurs. It is assumed that this load step change is followed by an identical change of the reference speed. The step change of the reference speed and the responses of the three examined electrical drives are shown in Fig. 6. The rotor inertia is selected small so that fast changes of the rotor speed are possible. It should be stressed that the small inertia renders torque and speed resonances -because of the harmonics produced by the power converter- more possible. It is obvious from Fig. 6 that the responses of the three examined electrical drives are very satisfying. After about 0.5 sec steady state is reached. The permanent speed error is zero due to the use of PI controllers. However the power converter using voltage space vector modulation presents the smallest overshoot and it is the less oscillatory.

In Figs 7-9 the current space vector trajectories are shown. This is a way to evaluate the PWM schemes by visual inspection of the trajectories of the current in the complex plane. The harmonic content of a steady state trajectory is observed as the deviation from its fundamental component, with the fundamental trajectory describing a

circle. Although deviations in amplitude are easily discernible, differences in phase are of equal significance. It should be stressed that the harmonic currents determine the copper losses which account for the major portion of the machine losses. The voltage space vector modulator operates at a switching frequency of 4 kHz while the sinusoidal pulse width modulator uses a carrier signal of 3.75 kHz. The used hysteresis band is 0.05 p.u. of the base current. The hysteresis current technique produces obviously the higher harmonic distortion. In case of the hysteresis current control scheme the used hysteresis band, the motor equivalent reactance and the dc voltage affect the switching frequency, and consequently the current harmonic content. Tuning the previous parameters the current harmonic content can be optimally adjusted. The harmonic content of the current in case of voltage space vector modulator can be further decreased using an optimal modulation method [20]-[22].
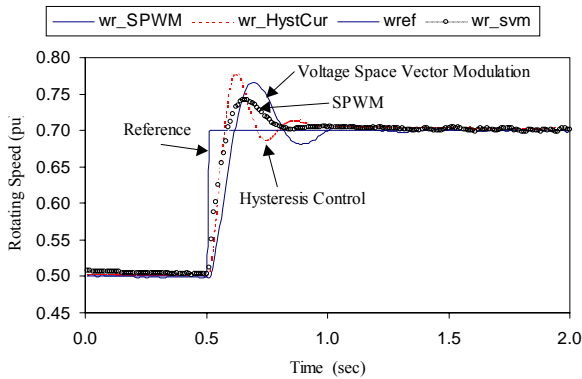

Fig. 6   Reference and actual rotating speeds for the three types of converters
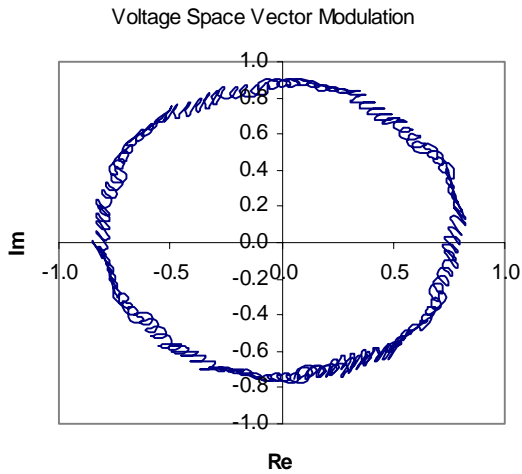

Fig. 7   Current trajectory of the converter using voltage space vector modulation technique.

In Fig. 10 the spectral densities of the steady-state electromagnetic torques of the three examined electrical drives are shown. In case of the hysteresis current controller three peaks at 13, 27, 41 Hz occur while the respective peak values in case of voltage space vector modulator are 10, 21 and 28 Hz. In case of SPWM technique a major peak occurs at 35 Hz and is result of the use of non-synchronized

carrier and modulation signals. The observed peaks depend on the used switching frequency, hysteresis band, the sampling technique and obviously on the use or not of a synchronization technique. The estimation of the peak values of the electromagnetic torque spectral density, is very useful as undesirable mechanical resonances [16]-[18] can be avoided if the natural frequencies of the induction machine and the mechanical drive are known.
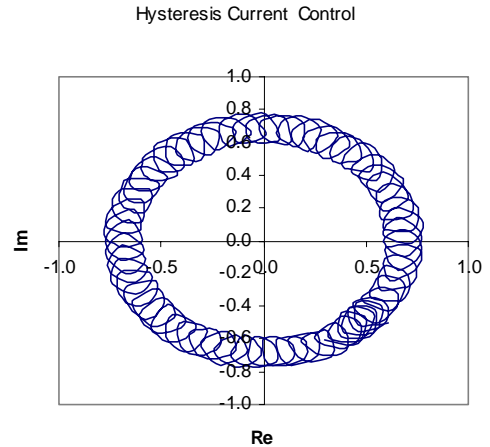

Fig. 8   Current trajectory of the converter using hysteresis current control.
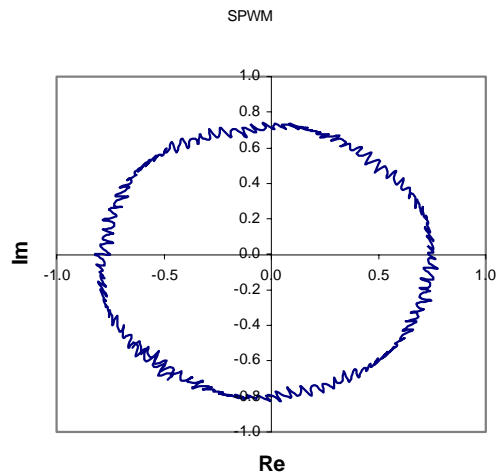

Fig. 9   Stator current trajectory of the converter using SPWM modulation technique.
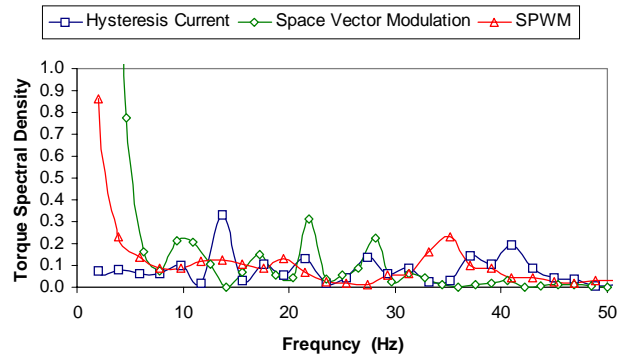

Fig. 10   Torque spectral density in the 0-50 Hz frequency area for the three power converters.
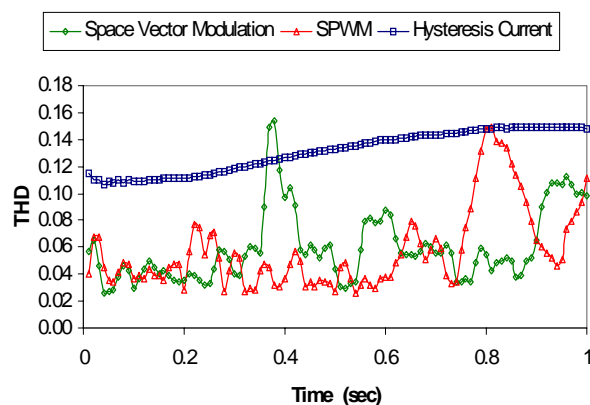
5

Fig. 11 THD for stator currents 1 sec before the disturbance.

In Fig. 11 the THD factor of the stator currents is shown in the time interval beginning 1 sec before the load and speed reference disturbances. THD is a mean of evaluating the current harmonic content and consequently the machine copper losses.

VI. CONCLUSIONS

In this paper, the dynamic performance of three of the most promising types of voltage source converters, is studied. The converters supply squirrel cage induction machines and they employ hysteresis current control, voltage space vector modulation and sinusoidal pulse width modulation, respectively. Detailed models for the electrical drives are used, allowing the study of their behavior in a broad bandwidth. The presented models are developed using Matlab code and Simulink. Vector control is used for the regulation of the rotor speed and the stator flux. In case of SPWM and voltage space vector modulation, an indirect field-oriented voltage controller is applied. The hysteresis current controller is composed of three independent per phase current controllers. The operational characteristics of the proposed variable speed schemes are studied showing a very satisfactory dynamic response. The hysteresis current controller produces the highest harmonic content and ohmic losses as seen from current trajectories and the obtained THDs. Using the steady state torque spectral densities conclusions can be drawn about possible mechanical resonances. It is shown that mechanical resonances can possibly occur at 10, 13 Hz for voltage space vector modulation and hysteresis current control technique.

REFERENCES

[1] Wilson, T.G., *"The evolution of power electronics"*, *IEEE Trans. Power Electronics*, Vol. 15, no 3 , pp. 439 –446, May 2000.
[2] Chan, C.C., Chau, K.T., "An overview of power electronics in electric vehicles ", *IEEE Trans. on Ind. Electronics*, vol. 44 no 1, pp. 3 –13, Feb. 1997.
[3] Novotny D.W., Lipo T.A., "Control and Dynamics of AC machines", Oxford Press, New York 1996.
[4] W. Leonard, "Control of Electrical Drives", Springer-Verlag, 1985.
[5] B.K. Bose, "Power Electronics and AC Drives", Prentice Hall, 1986.
[6] B.K. Bose, "Power Electronics and Variable Frequency Drives – Technology and Applications", IEEE Press, New York, 1997.
[7] El Moucary C., Mendes E., Razek A., "Decoupled direct control for PWM inverter-fed induction motor drives", *IEEE Trans. Ind. Appl.*, vol. 38, no 5, pp. 1300-1315, Sept- Oct. 2002.
[8] *J. Holtz* , "Pulse Width Modulation for Electronic Power Conversion", Proceedings of the IEEE, vol. 82, No. 8, August 1994.
[9] F.D. Kanellos, N.D. Hatziargyriou, "The Effect of Variable Speed Wind Turbines on the Operation of Weak Distribution Networks", to be published in *IEEE Trans. Energy Conversion*, vol. 17, no. 4, December 2002.
[10] Chee-Mun Ong, "Dynamic Simulation of Electric Machinery using Matlab/Simulink", Prentice Hall PTR, 1998.
[11] F.D. Kanellos, N.D. Hatziargyriou "A new proposed Control Scheme for Wind Turbines using Neural Networks", PES Winter Meeting 2002, New York.
[12] P.C. Krause, "Analysis of Electric Machinery", McGraw-Hill, 1986.
[13] D.M. Brod and D.W. Novotny, "Current Control of VSI-PWM Inverters", IEEE Trans. Ind. Appl., vol. IA-21, no. 3, pp. 562-570, May-June 1985.
[14] Holtz J., Beyer B. , "Fast current trajectory tracking control based on synchronous pulse width modulation", *IEEE Trans. Ind. Appl.*, 1995.
[15] Schauder C.D., Caddy R., "Current control of voltage source inverters for fast four-quadrant drive performance", *IEEE Trans. Ind. Appl.*, vol. IA-18, no. 2, pp. 163-171, March-April 1982.
[16] Lipo T.A., Krause P.C.. Jordan H.E.*, "Harmonic torque and speed pulsations in a rectifier-inverter induction motor drive", *IEEE Trans. Power App. Syst.*, vol. PAS-88, pp 579-587, May 1969.
[17] Tinghsu Su, Hattori S., Ishida M., Hori T.*, "Suppression control method for torque vibration of AC motor utilizing repetitive controller with Fourier transform", *IEEE Trans. on Ind. Appl.,* vol. 38, no 5, pp. 1316 –1325, Sept.-Oct. 2002.
[18] Shaotang Chen, Namuduri C., Mir S., "Controller-induced parasitic torque ripples in a PM synchronous motor", *IEEE Trans Ind. Appl.,* vol. 38, no 5, pp. 1273 –1281, Sept.-Oct. 2002.
[19] Narayanan G., Ranganathan V.T., "Extension of operation of space vector PWM strategies with low switching frequencies using different overmodulation algorithms", *IEEE Trans. Power Electronics*, Vol. 17, no 5 , pp. 788 –798, Sept. 2002.
[20] Kolar J. W., Ertl H., Zach F. C., *"Influence of the modulation method on the conduction and switching losses of a PWM converter system" IEEE Trans. Ind. Appl.*, vol. 27, no. 6, pp. 1063-1075, November-December 1991.
[21] Patel H. S., Hoft R.G. "Generalized techniques of harmonic elimination and voltage control in thyristor converters", *IEEE Trans. Ind. Appl.*, vol. IA-9, no. 3, pp. 310-317, May-June 1973.
[22] Buja G. S., Indri G. B., "Optimal pulse width modulation for feeding AC motors", *IEEE Trans. Ind. Appl.*, vol. IA-3, no. 1, pp. 38-44, January-February 1977.

Author Biographies

F.D. Kanellos received his Electrical and Computer Engineering degree at National Technical University of Athens, in 1998. He is PhD student in the Electrical Engineering Department of NTUA. His research interests include power electronics and also modeling and control of variable speed wind turbines.
N.D. Hatziargyriou is Professor at Power Division of the Electrical Engineering Department of NTUA. His research interests include Renewable, Dispersed Generation, Dynamic Security and AI techniques. He is member of CIGRE SCC6 and senior member of the IEEE.